Optical Emission Study of Radio-Frequency Excited Toluene Plasma

Szetsen Lee,* Shiao-Jun Liu, and Rui-Ji Liang

Department of Chemistry and Center for Nano-technology, Chung Yuan Christian University, Jhongli, Taoyuan, 32023, Taiwan

Received: August 10, 2008; Revised Manuscript Received: October 24, 2008

UV−visible emission spectra of radio-frequency (rf) excited toluene plasma were studied. Benzyl radicals as well as toluene monomer and excimer were observed in toluene plasma. It was found that the intensities, peak positions, and linewidths of monomer and excimer emission bands exhibit strong dependence on rf power and plasma processing time. This can be ascribed to photochemical reactions in plasma. Gas-chromatographic analysis of the deposition products from toluene plasma indicated that the main component was bibenzyl. Spectroscopic evidence has shown that the bibenzyl molecule was formed by the coupling reaction between two benzyl radicals in plasma. The spectroscopic characteristics of toluene monomer and excimer are correlated with a kinetic model in plasma.

1. Introduction

The removal of industrial toxic gases such as volatile organic compounds (VOCs) has been an environmental issue of primary concern. Nonthermal plasma technique has been proved to be one of the effective ways of decomposing VOCs, such as toluene,[1] benzene,[2] and acetone.[3] However, it is found that plasma treatment can lead to the formation of a diversity of byproducts.[4,5] Whether these byproducts can have an impact on the environment still remains an issue.

Plasma provides an environment of photons, electrons, and ions with a wide distribution of energies. The photochemical and electron impact effects in plasma may produce effects similar to conventional UV-irradiation experiments.[6,7] It is known that benzyl radical can be produced from toluene under UV radiation[8−10] or by discharge.[11−16] It has been proposed that predissociation is the main pathway for the formation of benzyl radical.[9] However, vacuum-ultraviolet (VUV) flash photolysis study has shown that the formation of benzyl radicals is from the vibrationally hot toluene molecules with efficient internal conversion.[10] The steady-state Hg-sensitized photolysis of toluene vapor has shown that phenyl radical is present in the products.[17] This process is also considered to be via a hot-molecule mechanism.

Toluene excimers have been observed in concentrated solutions[7,18−21] and supersonic molecular jets.[22,23] On the other hand, among the known works related to the spectroscopic studies of benzene and alkylbenzene plasmas,[11−16] there is no report or clear indication on the observation of toluene excimer in discharges. In this study, we have observed benzyl radicals as well as the power- and time-dependence of toluene monomer and excimer fluorescence in a radio-frequency (rf) discharge.

The goal of this study is to elucidate the reaction mechanisms of the conversion of toluene in plasma to byproducts with controllable distribution. Understanding the chemical reaction pathways leading to destruction of VOCs and formation of less environmentally harmful byproducts is an essential subject of study.

* To whom the correspondence should be addressed. E-mail: slee@cycu.edu.tw.

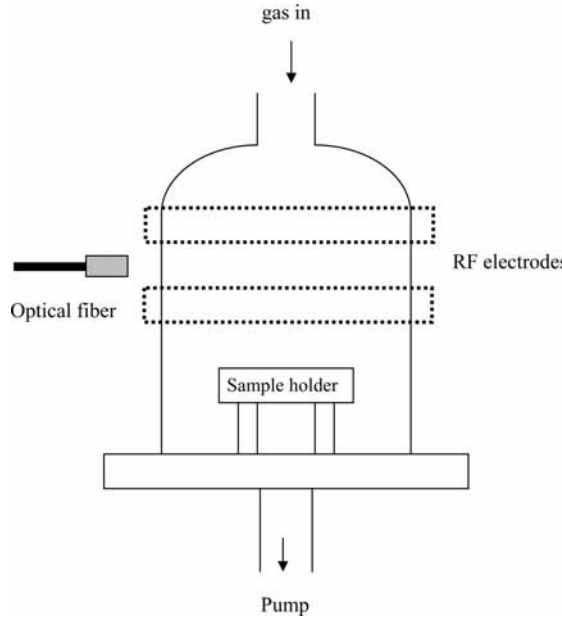

Figure 1. Toluene plasma deposition and optical emission setup.

2. Experimental Section

Pure toluene plasma was generated with an rf power source (Hüttinger, 13.56 MHz) in a glass bell jar of 8 in. diameter. The ring-shaped copper electrodes (width ∼ 1 cm) were wrapped around the glass bell jar with 5 cm distance between cathode and ground (Figure 1). A bubbler containing toluene (Aldrich, ≥99.9%) was connected to the bell jar for sample feeding. The vapor pressure of toluene in the bell jar was kept around 1 Torr. The rf power was adjusted between 50 and 250 W for typical deposition and optical emission experiments. A stainless steel plate (3 in. diameter) inside the bell jar was used to receive deposition products from toluene plasma. Optical emission from the plasma was directed to a scanning monochromator (Jobin Yvon, 600 lines/mm, blazed for 330 nm) by an optical fiber. The signal was amplified by a TE-cooled CCD (Jobin Yvon, 1024 × 256 pixels). The slit width was fixed at 0.01 mm. The exposure time was varied from 500 ms to 10 s to improve the signal-to-noise ratio.

10.1021/jp807139x CCC: $40.75
Published on Web 12/02/2008

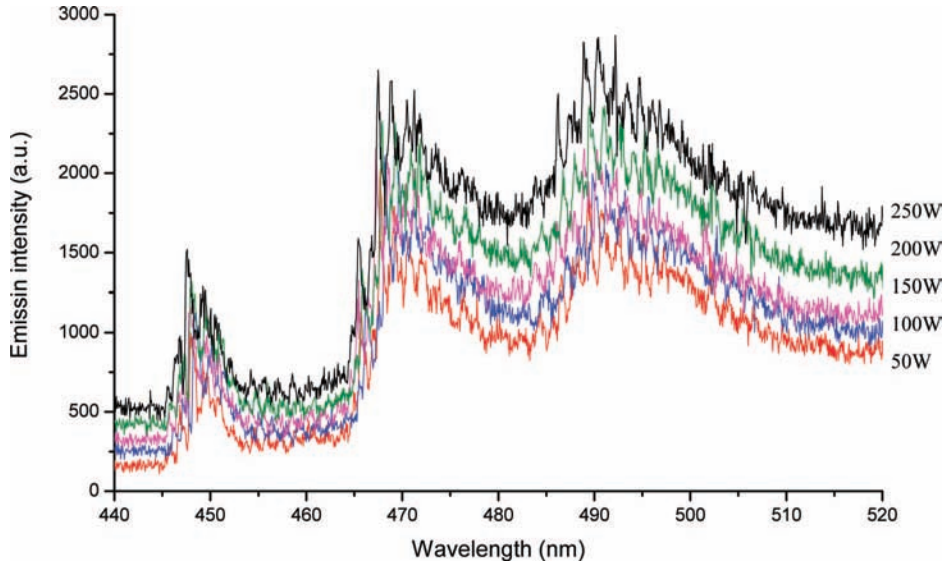

Figure 2. Optical emission spectra of benzyl radicals between 445 and 500 nm.

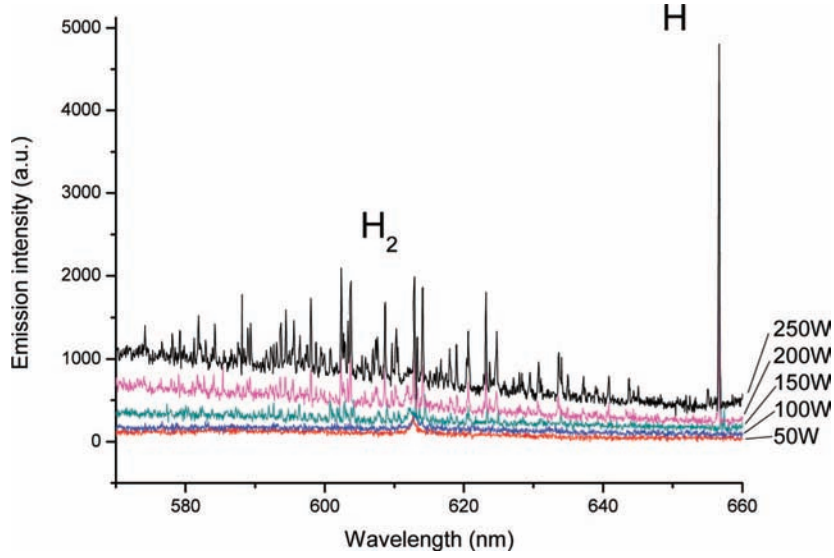

Figure 3. Optical emission spectra of hydrogen (H and H_2) in toluene plasma.

Oily deposition collected from the stainless steel plate was dissolved in benzene and separated by gas chromatography/mass spectrometry (GC/MS) (Agilent Technologies, GC-5890, MS-5973). Chromatogram and mass peak distribution of products in the filtrate were compared with retention times and fragment patterns of standard database.

3. Results and Discussion

3.1. Optical Emission Spectra. The optical emission spectrum (OES) of benzyl radicals is shown in Figure 2. It clearly shows that the emission band intensities between 445 and 500 nm, corresponding to $\tilde{X}^2B_2 \leftarrow \tilde{B}^2B_2$ and $\tilde{X}^2B_2 \leftarrow \tilde{A}^2A_2$ transitions,[24] increase with rf power. Hydrogen (H and H_2) signals between 600 and 660 nm also grow with rf power (Figure 3). Figure 4 illustrates the rf power and time dependence of toluene emission profiles. The broad bandwidth of toluene emission is due to the fact that electrons are not monoenergetic.[7,18] Just like the concentration-dependence of the fluorescence spectra in solutions,[7,18−20] the quasi-continuous (13.56 MHz) electron bombardment in toluene plasma gives similar photochemical effects to irradiation with UV light.[6,7] As rf power gradually increases, the toluene monomer peak falls and the excimer peak emerges. The reaction pathways of toluene in plasma can be described as follows:

$$M + e^- \rightarrow M^* + e^-: \quad k_e n_e[M],\ k_e = AT_e^{\alpha} \exp(-\varepsilon/k_B T_e) \tag{1}$$

$$M^* \rightarrow M + h\nu_f: \quad k_f[M^*] \tag{2}$$

$$M + M^* \rightleftharpoons M_2^*, \quad \begin{matrix} k_{ex}[M][M^*] \\ k_r[M_2^*] \end{matrix} \tag{3}$$

$$M_2^* \rightarrow M + M + h\nu_{f'}: \quad k_{f'}[M_2^*] \tag{4}$$

$$M^* \rightarrow P: \quad k_p[M^*] \tag{5}$$

$$M_2^* \rightarrow P': \quad k_{p'}[M_2^*] \tag{6}$$

The toluene molecule (M) is excited by rf-driven electrons ($k_e n_e[M]$). In the Arrhenius expression of k_e, T_e is the electron temperature, which indicates the degree of excitation in plasma. The excited toluene molecule monomer (M*) can undergo fluorescent decay (k_f), association (k_{ex}) with a ground-state toluene molecule to form an excimer (M_2*), and nonradiative processes or reactions to products (k_p). M_2* can also undergo

fluorescent decay ($k_{f'}$), reverse of association reaction (k_r), and nonradiative processes or reactions to products ($k_{p'}$). The corresponding rate equations can be expressed as

$$\frac{d[M^*]}{dt} = k_e n_e[M] - k_M[M^*] + k_r[M_2^*] \quad (7)$$

$$\frac{d[M_2^*]}{dt} = k_{ex}[M][M^*] - k'[M_2^*] \quad (8)$$

where $k_M = k_f + k_p + k_{ex}[M]$ and $k' = k_{f'} + k_{p'} + k_r$ represent the total decay rates of monomer and excimer, respectively. The solutions of the above rate equations yield the power- and time-dependent concentrations of monomer and excimer.

$$[M^*] = \left[[M^*]_0 - \frac{k' k_e n_e[M]}{(k_M k' - k_{ex}[M])}\right] e^{-k_1 t} + \frac{k' k_e n_e[M]}{(k_M k' - k_{ex}[M])},$$

$$k_1 = \frac{(k_M + k_r k') + \sqrt{(k_M - k_r k')^2 + 4 k_r k_{ex}[M]}}{2} \quad (9)$$

$$[M_2^*] = \left[[M_2^*]_0 - \frac{k_{ex} k_e n_e[M]^2}{(k_M k' - k_r k_{ex}[M])}\right] e^{-k_2 t} + \frac{k_{ex} k_e n_e[M]^2}{(k_M k' - k_r k_{ex}[M])},$$

$$k_2 = \frac{(k_M + k') - \sqrt{(k_M - k')^2 + 4 k_r k_{ex}[M]}}{2} \quad (10)$$

For an infinitely dilute toluene plasma (i.e., $[M] = 0$), it is rather straightforward to show that $k_1 = k_M$ and $k_2 = k'$. $[M^*]_0$ and $[M_2^*]_0$ are the initial concentrations of monomer and excimer. In this work, toluene was quasi-continuously excited in an rf field. The scans of the emission spectra with different rf power settings were taken consecutively from 25 W to 150 W without turning off plasma. In fact, the initial concentration of the current run is approximately the final concentration of the preceding run. Because of such a particular experimental condition, the steady-state approximation of the concentrations of monomer and excimer does apply in the expression of the fluorescence quantum yields of monomer (ϕ_{M^*}) and excimer ($\phi_{M_2^*}$), instead, time-dependent expression should be considered:

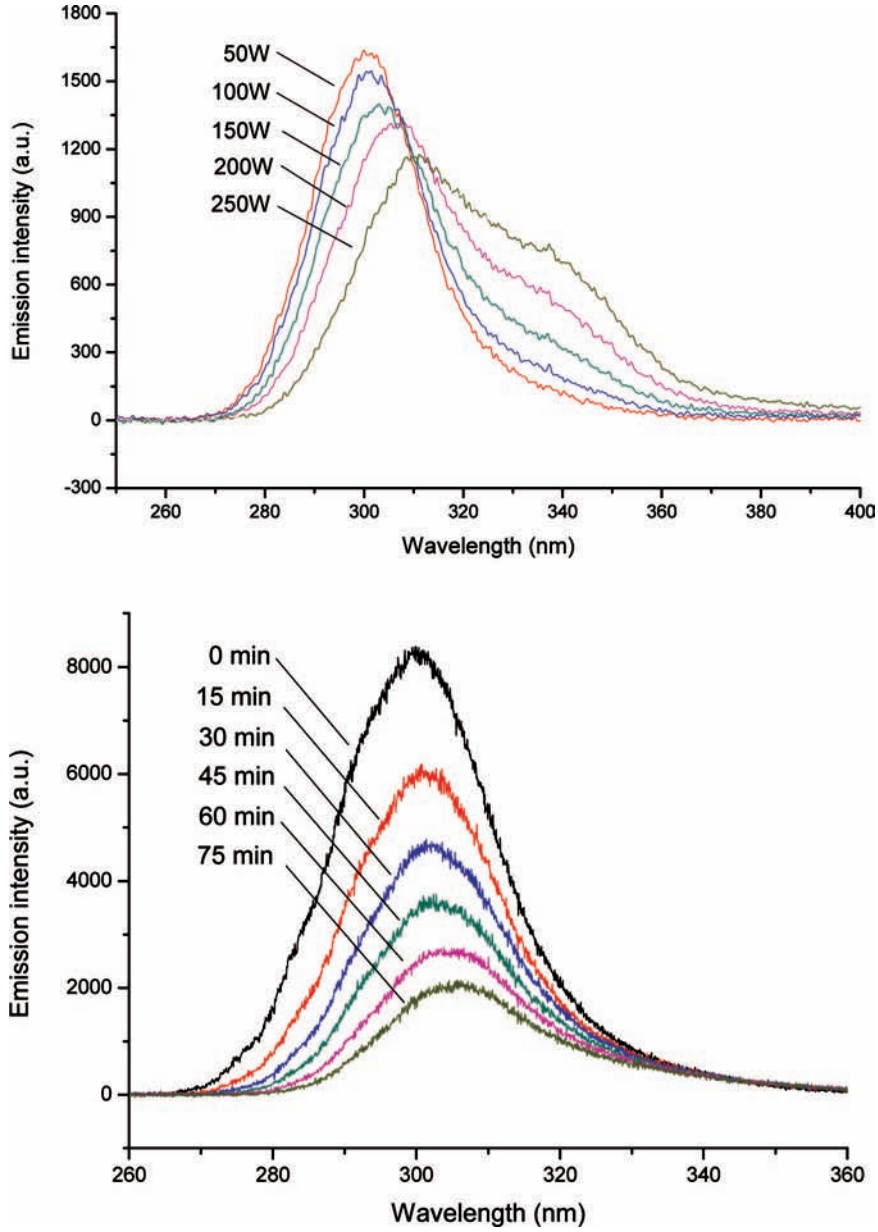

Figure 4. Power (top, integration time = 1s) and time (bottom, rf power = 50 W) dependence of toluene optical emission profiles.

$$\phi_{M^*} = \left[\frac{k_f[M^*]_0}{k_e n_e[M]} - \phi_{M^*,S}\right] e^{-k_1 t} + \phi_{M^*,S}$$

$$= \frac{k_f[M^*]_0 e^{-k_1 t}}{k_e n_e[M]} + (1 - e^{-k_1 t})\phi_{M^*,S} \quad (11)$$

$$\phi_{M_2^*} = \left[\frac{k_{f'}[M_2^*]_0}{k_e n_e[M]} - \phi_{M_2^*,S}\right] e^{-k_2 t} + \phi_{M_2^*,S}$$

$$= \frac{k_{f'}[M_2^*]_0 e^{-k_2 t}}{k_e n_e[M]} + (1 - e^{-k_2 t})\phi_{M_2^*,S} \quad (12)$$

where $\phi_{M^*,S} = (k_f k')/(k_M k' - k_{ex}[M])$ and $\phi_{M_2^*,S} = (k_{f'} k_{ex}[M])/(k_M k' - k_r k_{ex}[M])$ are the steady-state fluorescent quantum yields of monomer and excimer.

3.1.1. Intensity Trend. Under fixed rf power, the time-dependence of the fluorescence intensities of monomer and excimer obey the first-order rate law (Figure 5). The fitted rate constants k_1 and k_2 with eqs 11 and 12 are found to be power-dependent. It shows that the decay rate of excimer (k_2) is very small compared to that of monomer (k_1) at low rf powers ($\leq$100 W). At high rf power (150 W), both k_1 and k_2 rise appreciably. If the rf power is further increased from 150 W to 250 W, the emission profiles become complicated. The monomer peak in the UV region gradually disappears and a new weak peak emerges in the visible region. The conversion from singlet-state excimer to triplet-state excimer has been observed in liquid toluene under intense electron impact.[7] OES shows that the degree of dissociation of toluene to benzyl radical and hydrogen atom is proportional to rf power (Figures 2 and 3). Therefore, the power dependence of rate constants k_1 and k_2 can be ascribed to nonradiative processes or chemical reactions (k_p and $k_{p'}$).

If the scanning interval for each spectrum is $\Delta\tau$ (typically around 2 min), then the fluorescence quantum yields of monomer and excimer can be approximated as

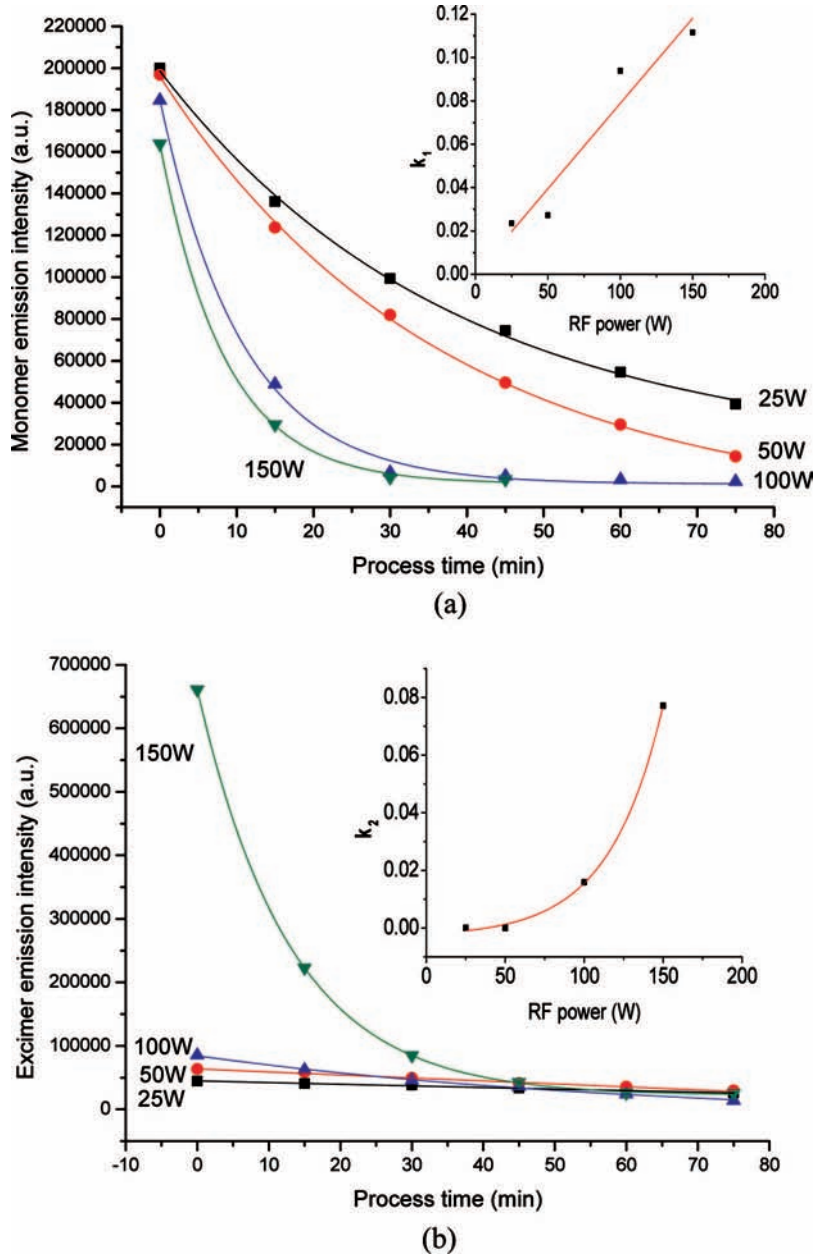

Figure 5. Time-dependent trends of (a) monomer and (b) excimer emission intensity. The power-dependence of the fitted decay rate constants k_1 and k_2 are illustrated in the inset.

$$\phi_{M^*} = \frac{k_f[M^*]_0 e^{-nk_1\Delta\tau}}{k_e n_e[M]} + (1 - e^{-nk_1\Delta\tau})\phi_{M^*,S} \quad (13)$$

$$\phi_{M_2^*} = \frac{k_{f'}[M_2^*]_0 e^{-nk_2\Delta\tau}}{k_e n_e[M]} + (1 - e^{-nk_2\Delta\tau})\phi_{M_2^*,S} \quad (14)$$

where n stands for the nth successive scan. Because the coefficients in eqs 13 and 14 depend on $nk_i\Delta\tau$ in the exponents which vary with the scanning time sequence, the exponential trend of the power-dependence of fluorescence intensity (Figure 6a) can therefore be interpreted. Implicitly, it is still a time-dependence effect.

3.1.2. Peak Position Trend. The emission peak positions of both monomer and excimer red-shift with increasing rf power (Figure 6b), which can be ascribed to the effect of photochemical reactions.[25] As rf power increases, the distribution of population shifts to higher excited states, which are more reactive than lower states. Therefore, the shorter wavelength portion of the fluorescence profile becomes weaker due to the disappearance of monomer and excimer through conversions to products. Likewise, the observed time-dependent red-shift of the peak positions is also due to chemical reactions (Figure 7). At higher rf powers (>150 W) and longer process time (>45 min), the monomer peak in the UV region becomes too weak to be measured. The emission profile is dominated by excimer and a new peak. The newly emerged peak in the visible range (410−475 nm), as discussed in the last paragraph, could be regarded as a manifestation of the triplet-state excimer[7] or the charge-transfer (CT) interaction.[22]

3.1.3. Linewidth Trend. The opposite line width (fwhm) trends of monomer and excimer with rf power (Figure 6c) can be explained by the pressure-broadening relation[26]

$$\Delta\lambda = \frac{\lambda^2 N\sigma\langle v\rangle}{c\pi} \quad (15)$$

where λ is the emission wavelength, N is the number density, σ is the collision cross-section, and $\langle v\rangle$ is the mean relative velocity of the emitting molecule. Since $\Delta\lambda$ is proportional to N and λ^2, the trend in Figure 6c is a combined result of the intensity and peak position relations in Figures 6a and 6b. Thus, $\Delta\lambda$ of monomer decreases slightly, but excimer increases with increasing rf power. Figure 8 illustrates the time-dependence trends of monomer and excimer $\Delta\lambda$. The decrease of $\Delta\lambda$ is not significant until rf power ≥ 100 W. It shows that the time-dependent change is mainly influenced by the decrease of number density due to chemical reactions and nonradiative processes.

3.2. Gas Chromatographic Analysis. GC/MS analysis (Figure 9) has shown that the composition of the oily deposition from toluene plasma is mainly bibenzyl and a small amount of stilbene and other benzene derivatives. Polycyclic aromatic hydrocarbons (PAHs) were virtually undetectable. Several peaks with mass numbers that matched certain types of compounds in the chromatogram, but the corresponding mass spectrum quality were very poor. No matter what the rf power is, bibenzyl and stilbene are always the dominant products in the deposition.

3.3. Bibenzyl Formation in Plasma. Theoretical studies[23,27] have indicated that the minimum energy configuration of the toluene excimer is a stacked structure where the two aromatic rings are parallel to each other (distance = 3.8 Å), but the two methyl groups are located in opposite directions. This is a structure that minimizes repulsion due to the methyl groups. Therefore, the direct conversion of toluene excimer to bibenzyl via dehydrogenation is unlikely.

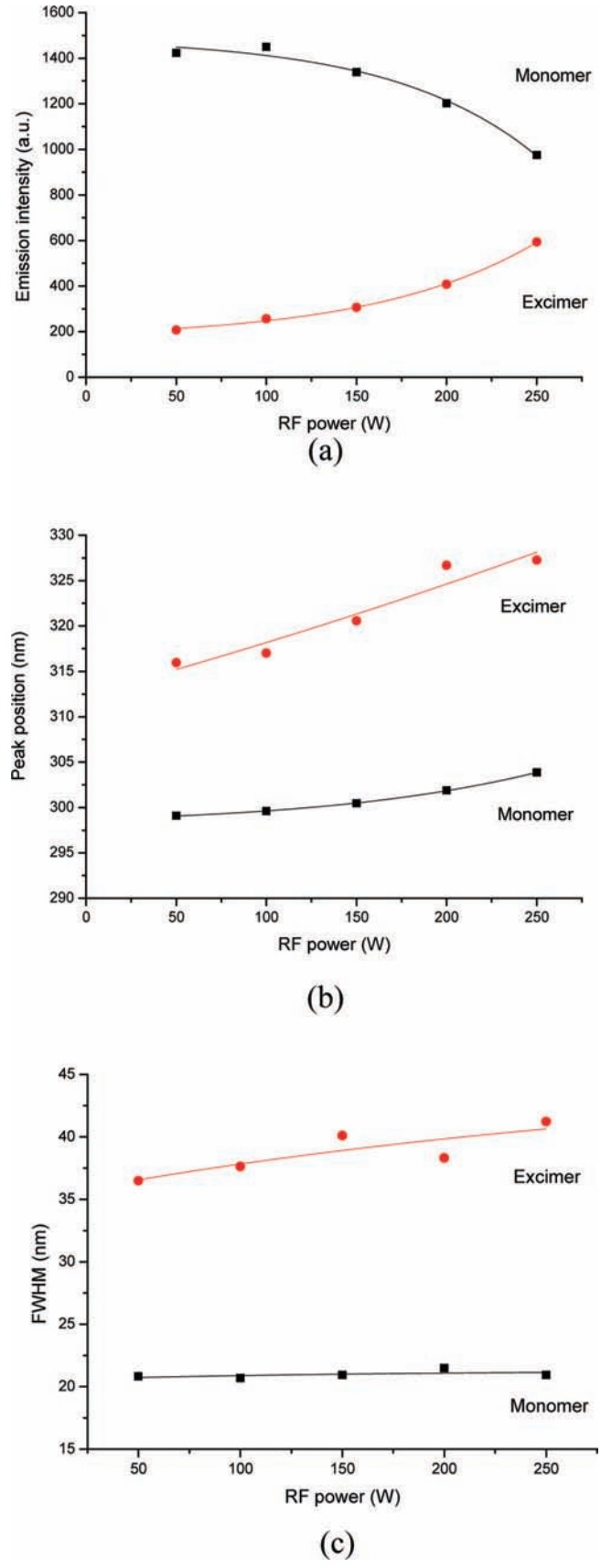

Figure 6. Power-dependent trends of monomer and excimer emission (integration time = 1 s): (a) intensity; (b) peak position; (c) fwhm.

With the supporting evidence from OES and GC-MS, the mechanism for bibenzyl formation can be understood. It is known that the dissociation of toluene to form benzyl radical

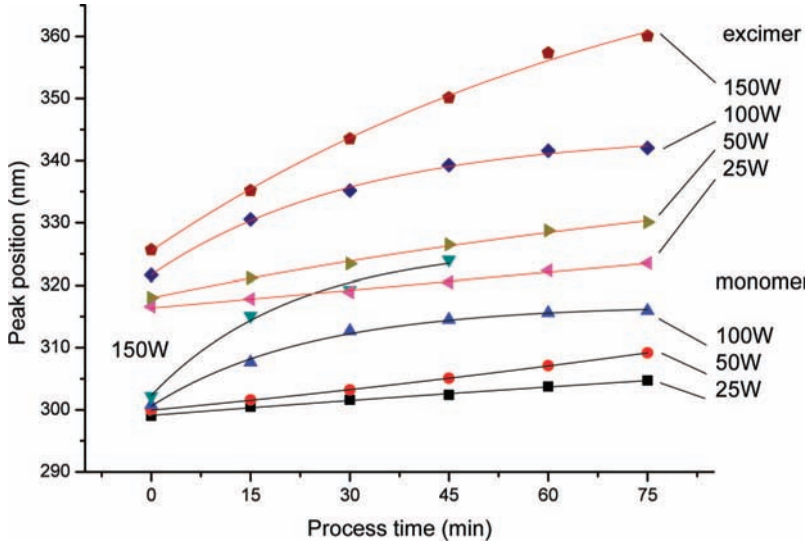

Figure 7. Time-dependent trends of monomer and excimer emission peak position.

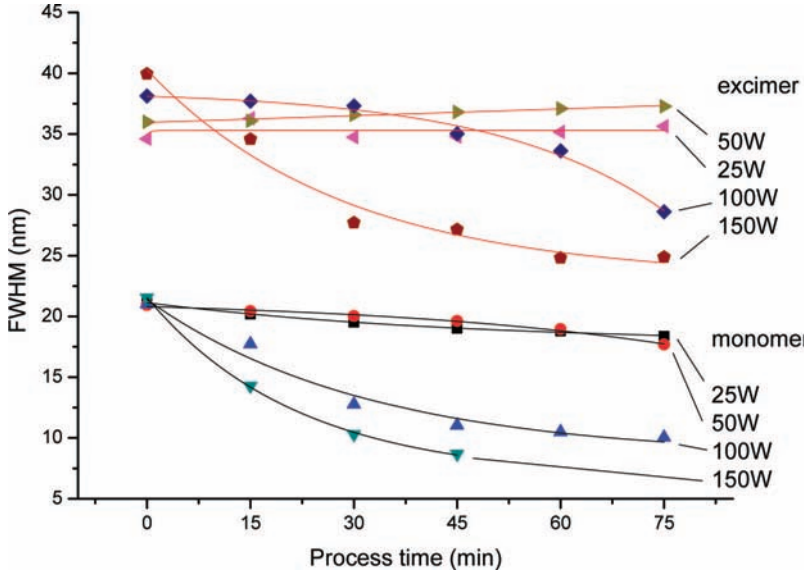

Figure 8. Time-dependent trends of monomer and excimer emission peak fwhm.

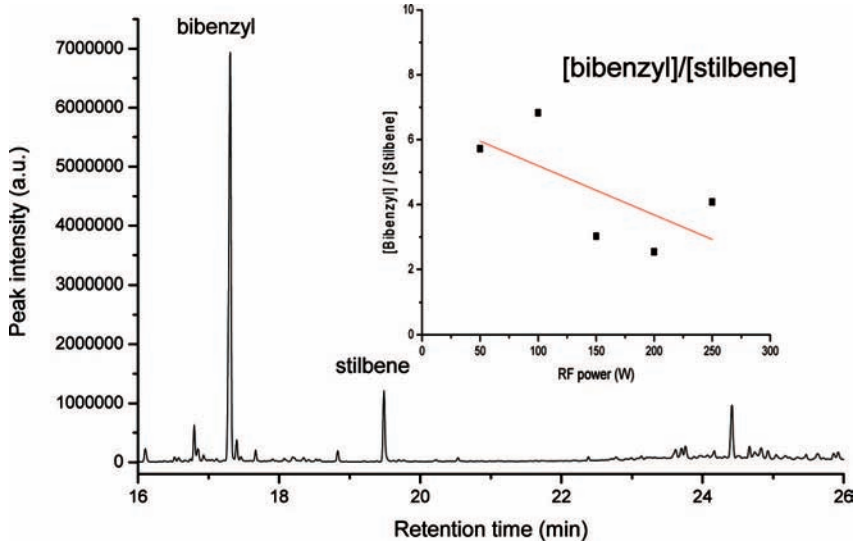

Figure 9. Chromatogram of toluene plasma deposition (rf power = 50 W). The inset shows the variation of the [bibenzyl]/[stilbene] ratio with rf power.

requires ~89 kcal/mol. The formation of phenyl radicals requires ~104 kcal/mol.[28] Almost all high temperature studies of the decomposition of toluene indicate that the formation of benzyl radicals, but not phenyl radicals, is favored.[29,30] From the OES of hydrogen (Figure 3), the rotational temperature of H_2 in toluene plasma is estimated to be 450 ± 25 K. Therefore, due to the abundance of benzyl radicals produced in cold toluene plasma, the coupling reaction between two benzyl radicals (activation energy ~0.45 kcal/mol)[31] is the main channel for producing bibenzyl.[32] It is similar to the formation of biphenyl from the recombination of phenyl radicals in benzene plasma.[33]

From the chromatographic analysis, it is found that as the rf power increases from 25 W to 150 W, not only the amount of deposition increases, but also the intensity ratio of bibenzyl and stilbene shifts from 5.7 to 4.1 (Figure 9, inset). It suggests that stilbene is produced from bibenzyl via dehydrogenation. This is supported by the OES evidence illustrated in Figure 3. It is worthwhile to mention that the high temperature kinetic study has shown that the formation of stilbene involves two steps. The bimolecular abstraction reaction between benzyl radical and bibenzyl forms toluene and a precursor $C_6H_5CHCH_2C_6H_5$ which is followed by dehydrogenation to stilbene and H.[34] Moreover, shock tube experiments have shown that the decomposition of the benzyl radical is faster than the decomposition of toluene proceeding with an activation energy around 80 kcal/mol. Apparently, the coupling of two benzyl radicals to form bibenzyl (activation energy ~0.45kcal/mol) is much faster than the decomposition of the benzyl radical.[31]

It is known that the LD50 value for bibenzyl is almost 5 times that of toluene. For stilbene, it is about 1.5 to 2 times more lethal than toluene.[35] Cold plasma treatment of toluene may have reduced some of the contamination issues due to toluene, but the environmental impacts due to bibenzyl and stilbene remain.

4. Conclusions

The results presented here are important in providing fundamental information required for understanding the reactions in toluene plasma. We have observed photochemistry-like behavior of toluene in a rf plasma. The power- and time-dependent variation of intensity, peak wavelength, and line width of the emission lines of monomer and excimer can be ascribed to the effect of nonradiative processes or chemical reactions. At high rf powers, chemical reactions as well as intersystem crossing processes become efficient. Cold rf plasma favors the formation of benzyl, but not phenyl or methyl phenyl radicals. Therefore, bibenzyl, but not PAHs, is the main composition of the deposition produced from the toluene plasma. The atomic hydrogen intensity is too weak and no other species can be used to determine T_e easily. Further work is being carried out by adding helium and argon to control plasma conditions such as T_e. It is hoped that the production of hazardous byproducts from toluene plasma can be reduced.

Acknowledgment. The authors would like to acknowledge the support from the National Science Council of Taiwan (NSC 96-2113-M-033-006-MY2) and the project of the specific research fields in the Chung Yuan Christian University (CYCU-95-CR-CH), the Ministry of Education, Taiwan.

Supporting Information Available: The derivation of various expressions of monomer and excimer is provided. This material is available free of charge via the Internet at http://pubs.acs.org.

References and Notes

(1) Yamamoto, T.; Ramanathan, K.; Lawless, P. A.; Ensor, D. S.; Newsome, J. R. *IEEE Trans. Ind. Appl.* **1992**, *28*, 528.
(2) Nunez, C. M.; Ramsey, G. H.; Ponder, W. H.; Abbott, J. H.; Hamel, L. E.; Kariher, P. H. *Control Technol.* **1993**, *43*, 242.
(3) Oda, T.; Yamashita, R.; Haga, I.; Takahashi, T.; Masuda, S. *IEEE Trans. Ind. Appl.* **1996**, *32*, 118.
(4) Oda, T.; Takahashi, T.; Yamaji, K. *IEEE Trans. Ind. Appl.* **2002**, *38*, 873.
(5) Urashima, K.; Chang, J.-S. *IEEE Trans. Dielect. Elect. Insulation* **2000**, *7*, 602.
(6) Suhr, H. *Angew. Chem., Int. Ed.* **1972**, *11*, 781.
(7) Christophorou, L. G.; Abu-Zeid, M.-E. M.; Carter, J. G. *J. Chem. Phys.* **1968**, *49*, 3775.
(8) Koyanagi, M.; Uejoh, K. *J. Lumin.* **1997**, *72−74*, 511.
(9) Porter, G.; Strachan, E. *Trans. Faraday Soc.* **1958**, *54*, 1595.
(10) Ikeda, N.; Nakashima, N.; Yoshihara, K. *J. Chem. Phys.* **1985**, *82*, 5285.
(11) Lortie, Y. *J. Phys. Radium* **1957**, *18*, 520.
(12) Schuler, H.; Stockburger, M. *Z. Naturforsch.* **1959**, *14a*, 229.
(13) Bindley, T. F.; Walker, S. *Trans. Faraday Soc.* **1962**, *58*, 217.
(14) Watts, A. T.; Walker, S. *J. Chem. Soc.* **1962**, *58*, 4323.
(15) Bieg, K. W. *Thin Solid Films* **1981**, *84*, 411.
(16) Selco, J. I.; Carrick, P. G. *J. Mol. Spectrosc.* **1989**, *137*, 13.
(17) Yamamoto, Y.; Takamuku, S.; Sakurai, H. *J. Phys. Chem.* **1970**, *74*, 3325.
(18) Carter, J. G.; Christophorou, L. G.; Abu-Zeid, M.-E. M. *J. Chem. Phys.* **1967**, *47*, 3879.
(19) Greenleaf, J. R.; Lumb, M. D.; Birks, J. B. *J. Phys. B* **1968**, *1*, 1157.
(20) Hirayama, F.; Lipsky, S. *J. Chem. Phys.* **1969**, *51*, 1939.
(21) Birks, J. B.; Braga, C. L.; Lumb, M. D. *Proc. R. Soc.* **1965**, *A283*, 83.
(22) Law, K. S.; Schauer, M.; Bernstein, E. R. *J. Chem. Phys.* **1984**, *81*, 4871.
(23) Saigusa, H.; Morohoshi, M.; Tsuchiya, S. *J. Phys. Chem. A* **2001**, *105*, 7334.
(24) Eidena, G. C.; Weisshaar, J. C. *J. Chem. Phys.* **1996**, *104*, 8896.
(25) Berlman, I. B. *Handbook of Fluorescence Spectra of Aromatic Molecules*; Academic Press: New York, 1965.
(26) Demtröder, W. *Laser Spectroscopy*, 2nd ed.; Springer-Verlag: Berlin, 1996.
(27) Chipot, C.; Jaffe, R.; Maigret, B.; Pearlman, D. A.; Kollma, P. A. *J. Am. Chem. Soc.* **1996**, *118*, 11217.
(28) Klippenstein, S. J.; Harding, L. B.; Georgievskii, Y. *Proc. Combust. Inst.* **2007**, *31*, 221.
(29) Rao, V. S.; Skinner, G. B. *J. Phys. Chem.* **1989**, *93*, 1864.
(30) Oehlschlaeger, M. A.; Davidson, D. F.; Hanson, R. K. *Proc. Combust. Inst.* **2007**, *31*, 211.
(31) Oehlschlaeger, M. A.; Davidson, D. F.; Hanson, R. K. *J. Phys. Chem. A* **2006**, *110*, 6649.
(32) Luther, K.; Oum, K.; Sekiguchi, K.; Troe, J. *Phys. Chem. Chem. Phys.* **2004**, *6*, 4133.
(33) Lee, S.; Chen, H.-F.; Peng, J.-W. *Plasma Chem. Plasma Process.* **2007**, *27*, 256.
(34) Frisch, S.; Hippler, H.; Troe, J. *Z. Physik. Chem.* **1995**, *188*, 259.
(35) The National MSDS Repository, http://www.msdssearch.com/.

JP807139X